SEEING AND THINKING

TOR VERGATA, 8-9 JUNE 2001

FUNCTIONAL ARCHITECTURE OF THE VISUAL CORTEX AND VARIATIONAL MODELS FOR KANIZSA'S MODAL SUBJECTIVE CONTOURS

Jean Petitot

CREA, Paris

petitot@poly.polytechnique.fr

INTRODUCTION

We will present a neuro-geometrical model for generating the *shape* of Kanizsa's modal subjective contours – that we will call in the following *K*-contours. It will be based on the functional architecture of the primary areas of the visual cortex.

As we are interested by a mathematical clarification of some very basic phenomena, we will restrict ourselves to a very small part of the problem, involving only the functional architecture of the first cortical area V1. We will see that the model is already quite sophisticated. Many other aspects (e.g., the role of V2) would have of course to be taken into account in a more complete model.

I. TOWARDS VARIATIONAL MODELS OF KANIZSA'S ILLUSORY CONTOURS

The object under study will not be classical straight *K*-contours but *curved* ones (*K-curves*) where the sides of the internal angles of the pacmen are *not aligned* (see figure 1).

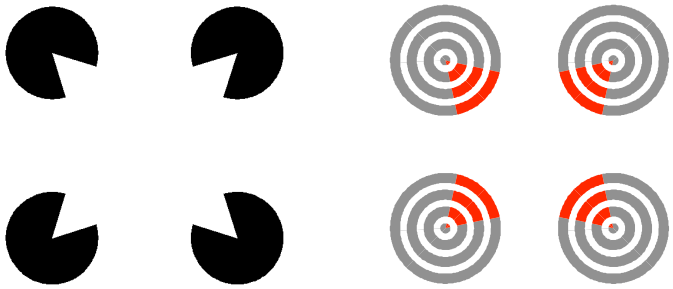

Figure 1. An example of a Kanizsa curved illusory modal contour. The second figure shows the well known "neon effect" (diffusion of color inside the area bounded by the virtual contours).

In an important paper, Shimon Ullman (1976) of the MIT AI Lab introduced the key idea of *variational models*.

> "A network with the local property of trying to keep the contours 'as straight as possible' can produce curves possessing the global property of minimizing total curvature."

He was followed by Horn (1983) who introduced a particular type of curves, the curves of least energy. Then in 1992, David Mumford introduced in computer vision, but only for *amodal* contours, a fundamental model based on the physical concept of *elastica*. Elastica are well known in classical Mechanics. They are curves minimizing at the same time the length and the integral of the square of the curvature κ, i.e. the energy

$$E = \int(\alpha\kappa+\beta)^2 ds$$

where ds is the element of arc length along the curve.

We will present here a slightly different variational model, based on the concept of "geodesic curves" in V1 and more realistic at the neural level. Let us begin with some experimental results.

II. AN EXPERIMENT ON *K*-CURVES (WITH JACQUES NINIO)

With our colleague Jacques Ninio of the Ecole Normale Supérieure (Paris) we worked out an experiment aiming at measuring the exact position of the extremum of a *K*-curve. For that purpose, we looked at families of *K*-curves sharing

2 configurations: triangle or square;

2 sizes of configuration;

2 sizes of pacmen;

4 orientations;

5 angles (see figure 2).

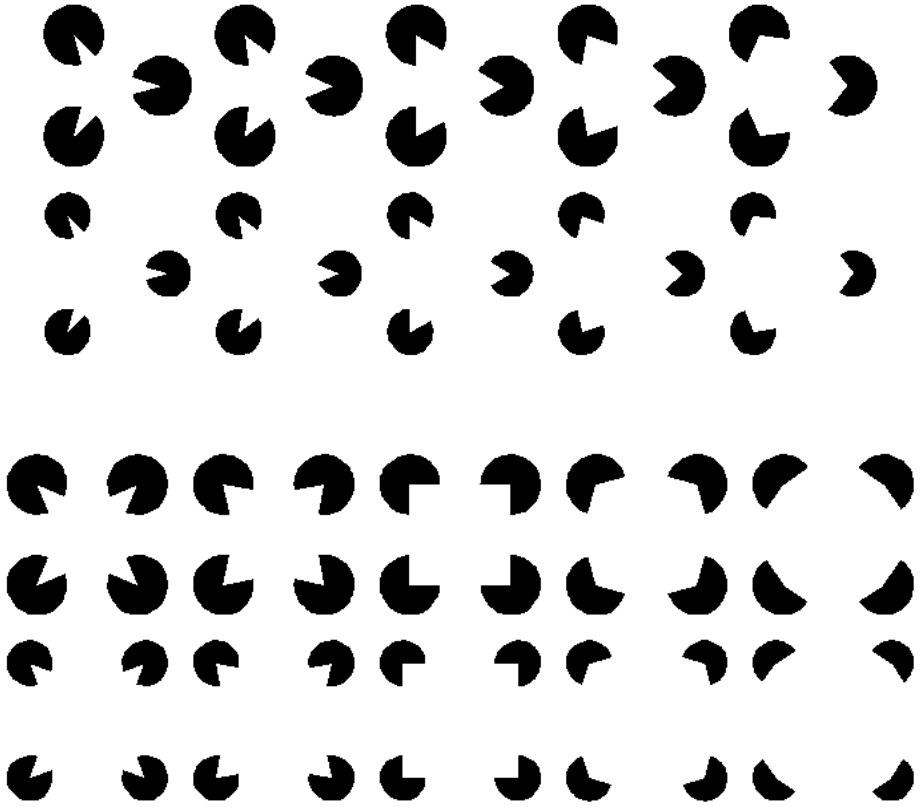

Figure 2. Curved Kanizsa triangles and squares used for the experiment with J. Ninio.

There are different methods for measuring the extremum of a *K*-contour. For instance, one can use the "subthreshold summation" method: the threshold for the detection of a small segment parallel to the *K*-contour decreases when the segment is exactly located on the *K*-contour (see figure 3).

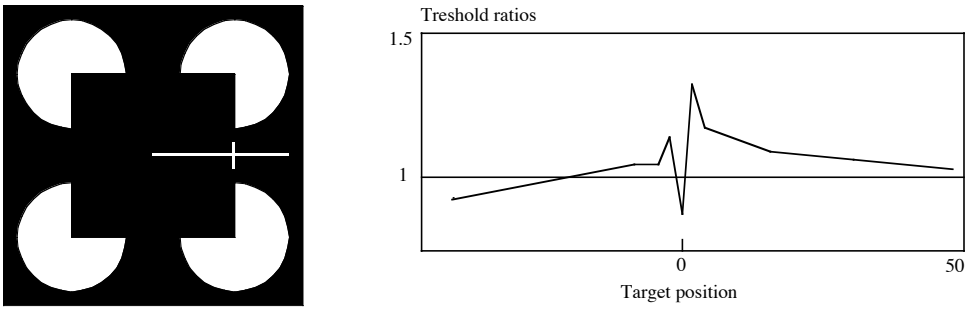

Figure 3. The subthreshold summation method: the threshold for the detection of a small segment parallel to the *K*-contour decreases when the segment is exactly located on the *K*-contour (from Dresp, Bonnet, 1955).

As for us, we used another method for detecting the extremal point of a *K*-curve: the subject was asked to place a marker (the extremity of an orthogonal line, a small segment, the symmetry axis of a small stripe) as exactly as possible at the extremum (see figure 4).

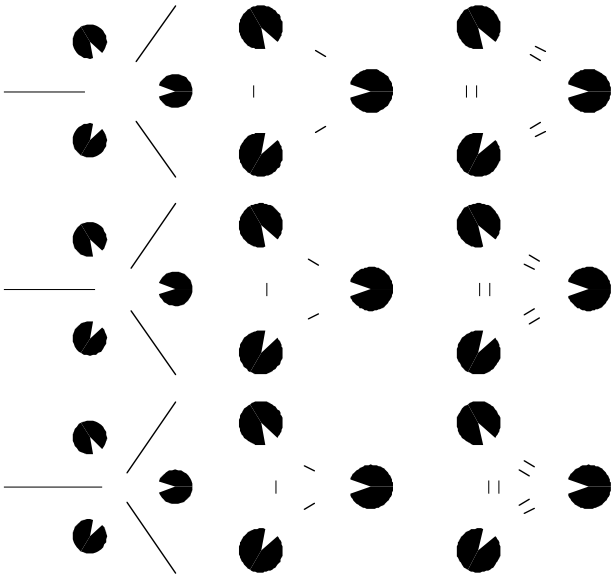

Figure 4. The method of detection of the extremal point of a curved *K*-contour. The subject is asked to place a marker (the extremity of an orthogonal line, a small segment, the symmetry axis of a small stripe) as exactly as possible at the extremum.

For different cases (triangle / square and small / large pacmen size) we compare three positions:

1. the piecewise linear position (intersection of the corresponding sides of the two pacmen);
2. the position chosen by the subjects;

3. the circle position (extremum of the arc of circle tangent to the sides of the two pacmen).

Let us take for instance the case (see figure 5) of the square with small pacmen (parameter *ps* = pacmen size = 1). The graphics plot the distance *d* of the extremum of the *K*-contour to the center of the configuration as a function of the aperture angle (figure 5b). *d* is measured by its ratio to the piecewise rectilinear case (which corresponds to $d = 1$) (figure 5a). 5 aperture angles are considered:

#2 corresponds to the classical case of a straight *K*-contour ($d_2 = 1$);

#1 to a slightly convex one ($d_1 > d_2 = 1$);

#0 to a more convex one ($d_0 > d_1 > d_2 = 1$);

#3 to a slightly concave one ($d_3 < d_2 = 1$);

#4 to a more concave one ($d_4 < d_3 < d_2 = 1$).

We see that the observed empirical *K*-contour is located between the piecewise rectilinear one and the circular one, and that the latter is therefore false.

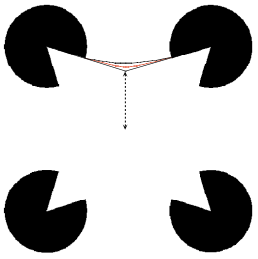

(a)

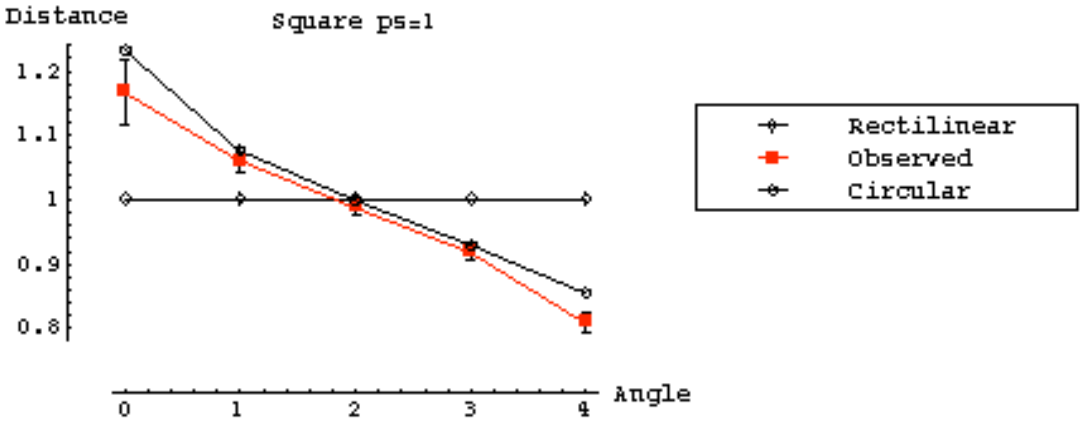

(b)

Figure 5. (a) The case of the square with small (parameter *ps* = pacmen size = 1) pacmen. The distance *d* is the distance of the extremum of the *K*-

contour to the center of the configuration. *d* is measured by its ratio to the piecewise rectilinear case (which corresponds therefore to $d = 1$). (b) Comparison of three *K*-contours: the piecewise rectilinear one, the one chosen by the subjects, the circle one. The graphics plots the distance *d* as a function of the aperture angle.

Another important result is that the deflections for the triangle and for the square are *not* the same. This is a typical *global* effect (see figure 6) which is very interesting but won't be taken into account here.

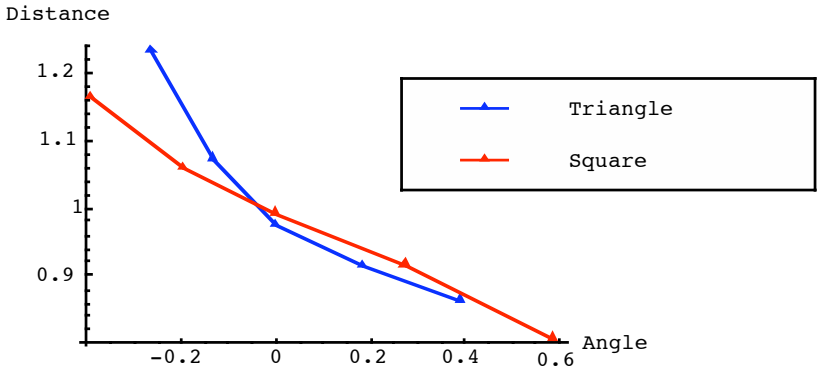

Figure 6. The deflections for the triangle and for the square are *not* the same.

III. NEURAL FUNCTIONAL ARCHITECTURE

We want now to work out a neurally plausible model of *K*-curves at the V1 level. We need first some results concerning the functional architecture of V1.

It is well known (see for instance De Angelis *et al*. 1995) that the receptive profile (the transfert function) of simple cells of V1 are like third order derivatives of Gaussians (with a well described underlying neural circuitry, from lateral geniculate body to layers of V1) (see figure 7).

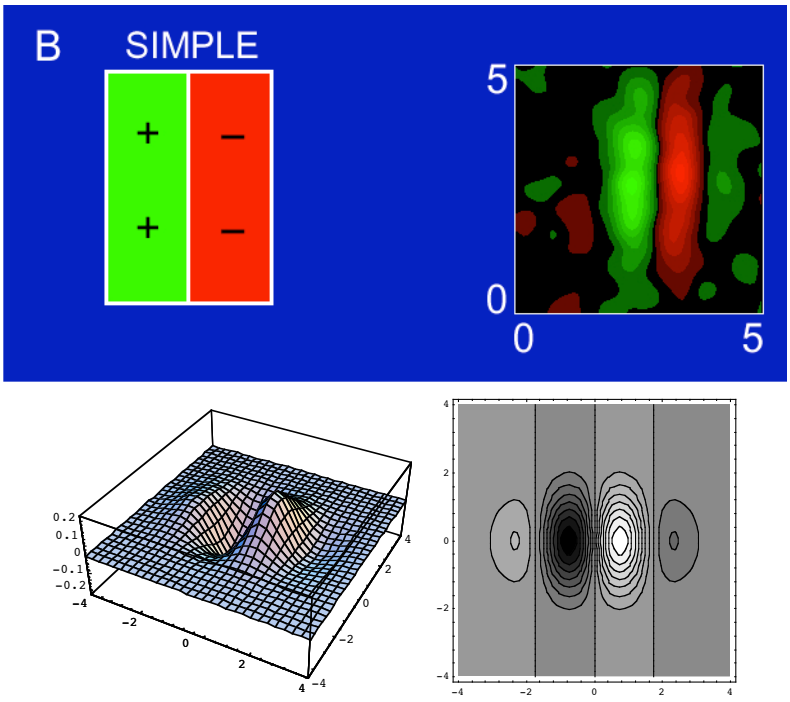

Figure 7. (a) Level curves of the receptive profile of a simple cell of V1 (right) and a simple schema of the receptive field (left) (from De Angelis *et al*. 1995). (b) A third derivative of a Gaussian along a direction. (c) The level curves. They fit very well with the empirical data (a).

Such receptive profile act on the signal as filters by convolution and process a *wavelet analysis*.

Due to their structure, the receptive fields of simple cells detect a *preferential orientation*. Simplifying the situation, we can say they detect pairs (a, p) of a spatial (retinal) position a and a local orientation p at a. They are organized in small modules called *hypercolumns* (Hubel and Wiesel) associating retinotopically to each position a of the retina R a full exemplar P_a of the space of orientations p at a. A very simplified schema of this structure (with a 1-dimensional base R) is shown at the figure 8. It is called a *fibration* of base R and fiber P.

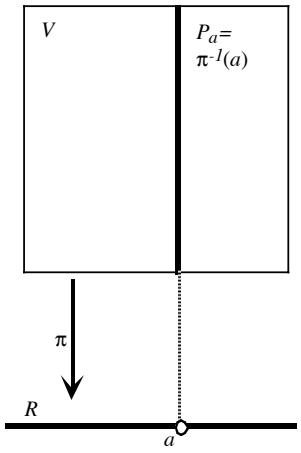

Figure 8. The general schema of a fibration with base space *R*, fiber *P* and total space *V*. The projection π projects *V* onto *R* and above every point *a* of *R* the fiber P_a is isomorphic to *P*.

Pairs (*a, p*) are called in geometry *contact elements*. But, beyond retinotopy formalized by the projection π, their set $V = \{(a, p)\}$ need to be *strongly structured* to allow the visual cortex to compute contour integration. We meet here the problem of the *functional architecture* of V1.

Recent experiments have shown that hypercolumns are geometrically organized in *pinwheels*. The cortical layer is reticulated by a network of singular points which are the centers of the pinwheels, around these singular points all the orientations are distributed along the rays of a "wheel", and the wheels are glued together in a global structure. The experimental method is that of in vivo optical imaging based on activity-dependent intrinsic signals (Bonhöffer & Grinvald, 1991) which allows to acquire images of the activity of the superficial cortical layers. Gratings with high contrast and different (e.g., 8) orientations are presented many times (20-80) with, e.g., a width of 6.25° for the dark strips and of 1.25° for the light ones, a velocity of 22.5°/s. A window is then opened above V1 and the cortex is illuminated with an orange light. One sums the images of V1's activity for the different gratings, constructs differential maps, and eliminates the low frequency noise. The maps are then normalized (by dividing the deviation relative to the mean value at each pixel by the global mean deviation) and the orientations are coded by colors (iso-orientation lines become therefore iso-chromatic lines).

In the celebrated figure 9 due to William Bosking, one can identify three classes of points:

1. regular points, where the orientation field is locally trivial;

2. singular points at the center of the pinwheels, where a full set of iso-orientation lines converge, two adjacent singular points being of opposed chiralities;

3. saddle-points at the center of the cells defined by the singular points.

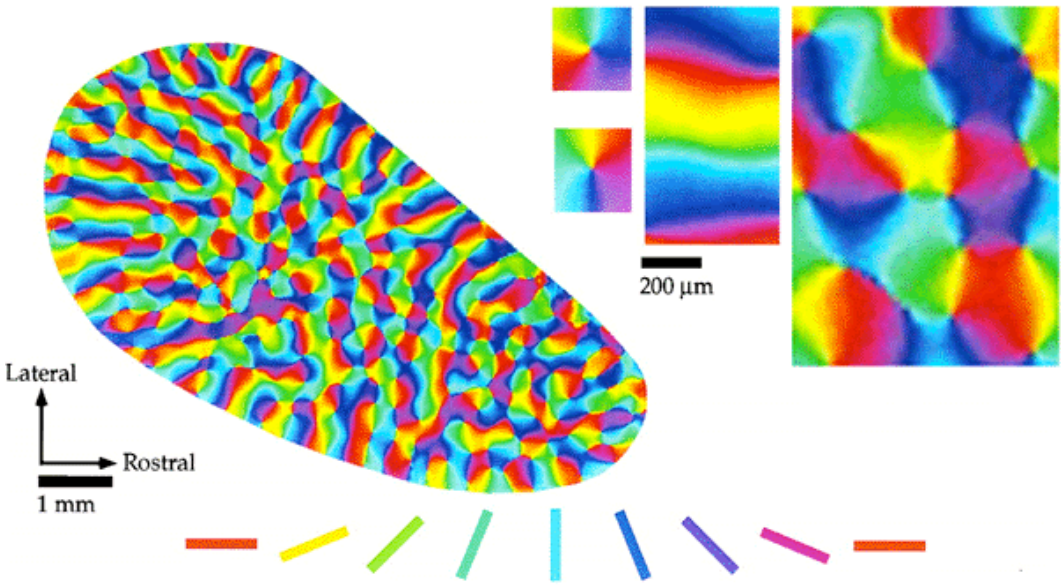

Figure 9. The pinwheel structure of V1 for a tree shrew. The different orientations are coded by colors. Examples of regular points and singularities of opposed chiralities are zoomed in. (From Bosking et al. 1997)

A cristal-like model of such a network of pinwheels is shown at the figure 10.

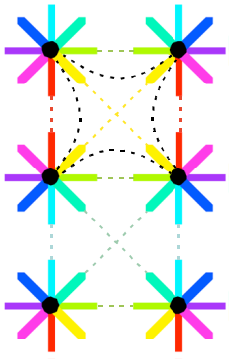

Figure 10. An idealized "cristal-like" model of pinwheels centered on a regular lattice of singular points. Some iso-orientations lines are represented. The saddle points in the centers of the domains are well visible.

As we have already noticed, the fonctional architecture associating retinotopically to each position a of the retina R an exemplar P_a of the space of the orientations implements a well known geometrical structure, namely the *fibration* $\pi : R \times P \rightarrow R$ with base R and fiber P. But such a "vertical" structure idealizing the retinotopic mapping between R and P is definitely insufficient. To implement a *global* coherence, the system must be able to *compare* between them two retinotopically neighboring fibers P_a et P_b over two neighboring retinal points a and b. This is a problem of *parallel transport* whose simplified schema is shown at the figure 11 (to be compared with figure 8). It has been solved experimentally by the discovery of *"horizontal" cortico-cortical connections*.

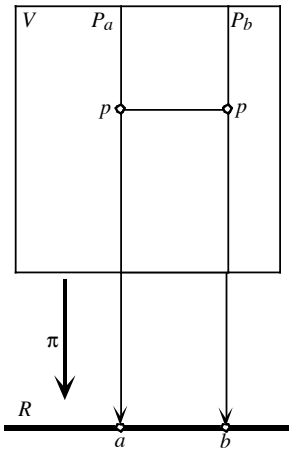

Figure 11. Cortico-cortical horizontal connections allow the system to compare orientations in two different hypercolumns corresponding to two different retinal positions a and b.

Experiments show that cortico-cortical connections connect neurons of the *same* orientation in neighboring hypercolumns. This means that the system is able to know, for b near a, if the orientation p at a is the same as the orientation q at b. The retino-geniculo-cortical "vertical" connections give an internal meaning to relations between contact elements (a, p) and (a, q) (*different* orientations p and q at the *same* point a) while the "horizontal" cortico-cortical connections give an internal meaning to relations between contact elements (a, p) and (b, p) (*same* orientation p at *different* points a and b) (see figure 12).

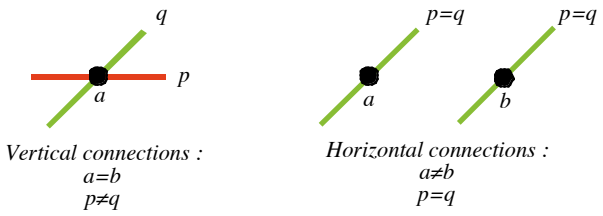

Figure 12. While the retino-geniculo-cortical "vertical'" connections give a meaning to the relations between pairs (a, p) and (a, q) (different orientations p and q at the same point a), the "horizontal'" cortico-cortical connections give a meaning to the relations between pairs (a, p) and (b, p) (same orientation p at different points a and b).

Moreover, as is schematized in figure 13, cortico-cortical connections connect not only parallel but also *coaxial* orientation cells, that is neurons coding contact elements (a, p) and (b, p) *such that p is the orientation of the axis ab*.

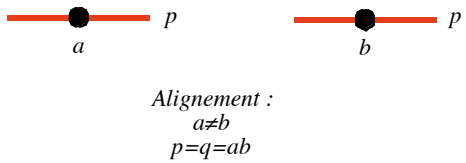

Figure 13

As emphasizes William Bosking (1997):

> "The system of long-range horizontal connections can be summarized as preferentially linking neurons with co-oriented, co-axially aligned receptive fields".

We will now show that these results mean that what geometers call the *contact structure* of the fibration $\pi : R \times P \to R$ is neurologically implemented.

IV. THE CONTACT STRUCTURE OF V1 AND THE ASSOCIATION FIELD

We work in the fibration $\pi : V = R \times P \to R$ with base space R and fiber P = set of orientations p. V is an idealized model of the functional architecture of V1. Mathematically, π can be interpreted as the fibration $R \times \mathbf{P}^1$ ($P = \mathbf{P}^1$ = projective line of orientations), or as the fibration

$R\times\mathbf{S}^1$ ($P = \mathbf{S}^1$ = unit circle of the orientation angles θ), or as the space $R\times\mathbf{R}$ of *1-jets* of curves C in R ($P = \mathbf{R}$ = the real line of the tangent $p = \tan(\theta)$ of the orientation angles). In the following, we will use the later model. A coordinate system for V is therefore given by triplets (x, y, p) where $p = \tan(\theta)$.

If C is a regular curve in R (a contour), it can be *lifted* to V through the map $\Gamma: C\rightarrow V = R\times P$ wich associates to every point a of C the contact element (a, p_a) where p_a is the *tangent* of C at a. Γ represents C as the *enveloppe* of its tangents (see figure 14).

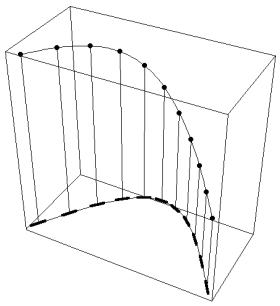

Figure 14. The lifting of a curve Γ, $y = f(x)$, in the base space R to the space V. Above every point $(x, y = f(x))$ of Γ we take the tangent direction $p = f'(x)$.

If $a(s)$ is a parametrization of C, we have $p_a = a'(s)$ (where a' symbolizes the derivative $y'(s)/x'(s)$) and therefore $\Gamma = (a(s), p(s)) = (a(s), a'(s))$. If $y = f(x)$ is a (local) equation of C, then a (local) equation of the lifting Γ in V is $(x, y, p) = (x, y, y')$.

To every curve C in R is associated a curve Γ in V. *But the converse is definitely false*. Indeed, let $\Gamma = (a(s), p(s))$ be a (parametrized) curve in V. The projection $a(s)$ of Γ is of course a curve C in R. But in general Γ *will not be* the lifting of its projection C. Γ will be the lifting of $C = \pi(\Gamma)$ *iff* $p(s) = a'(s)$. In differential geometry, this condition is called a Frobenius *integrability condition*. Technically, it says that to be a *coherent* curve in V, Γ must be an *integral curve* of the contact structure of the fibration π. We show in figure 15, besides the integrable example of figure 14, three exemples of *non* integrable curves Γ which are not the lifting of their projection C.

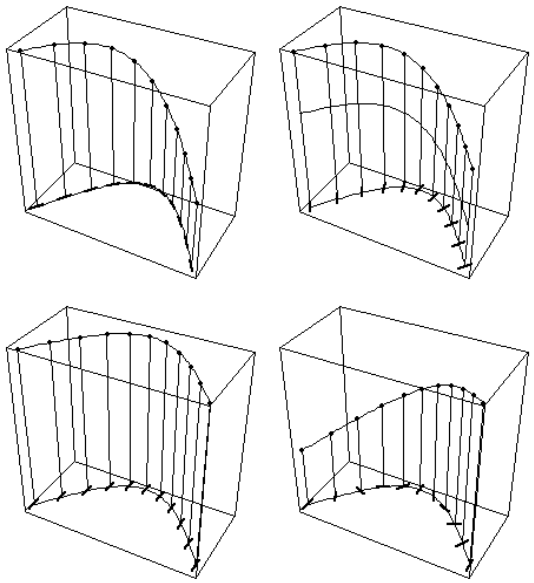

Figure 15. The association field as a condition of integrability. (a) The integrability condition is satisfied. (b), (c), (d) the condition is not satisfied. In (b) we add a constant angle to the tangent (i.e. $p = f'(x) + p_0$). In (c) p is constant while f' is not. In (d) p rotates faster than f'.

Geometrically, the integrability condition means the following. Let $t = (x, y, p; 1, y', p')$ be a tangent vector to V at the point $(a, p) = (x, y, p)$. If $p = y'$ we get $t = (x, y, p; 1, p, p')$. It is easy to show that this condition means exactly that t is in the *kernel* of the 1-form $\omega = dy - pdx$. This kernel is a plane, called the *contact plane* of V at (a, p), and the integrability condition for a curve Γ in V says exactly that Γ is tangent at each of its point (a, p) to the contact plane at that point. It is in that sense that Γ is an *integral curve* of the contact structure of V.

The integrability condition is a version of the Gestalt principle of "good continuation". Its psychophysical counterpart has been experimentally analyzed by David Field, Anthony Hayes and Robert Hess (1993) and explained using the concept of *association field*. Let (a_i, p_i) be a sequence of contact elements embedded in a background of distractors. The authors show that they generate a perceptively salient curve (pop-out) iff the p_i are *tangent* to the curve interpolating the a_i. This is due to the fact that the activation of a simple cell detecting a contact element (a, p) *pre*-activates via the horizontal cortico-cortical connections, cells detecting contact elements (c, q) with c roughly aligned with a in the direction p and q close to p. The pre-activation is strongly enhanced if the cell (c, q) is sandwiched between a cell (a, p) and a cell (b, p) (see figure 16)

Preactivation of a cell (c,p)

Figure 16.

The pop-out of the curve generated by the (a_i, p_i) is a typical Gestalt phenomenon which results from a *binding* induced by the co-activation. It manifests a very particular type of grouping. As was emphasized by Field, Hayes, and Hess (1993):

> "Elements are associated according to joint constraints of position and orientation." (p. 187)
>
> "The orientation of the elements is locked to the orientation of the path; a smooth curve passing through the long axis can be drawn between any two successive elements." (p. 181)

This is clearly a discrete version of the integrability condition.

V. A VARIATIONAL MODEL OF MODAL KANIZSA ILLUSORY CONTOURS

In such a framework, we can solve some aspects the Kanizsa problem in a *principled* way. Two pacmen of respective centers a and b with a specific aperture angle define two contact elements $A = (a, p)$ and $B = (b, q)$ of V. A K-curve interpolating between A and B is

1. a curve C from a to b in R with tangent p at a and tangent q at b;
2. a curve minimizing a sort of "energy" (variational problem).

But as far as the integration of C is processed in V, we must lift the problem to V. We must therefore find *in* V a curve Γ interpolating between (a, p) and (b, q) *in* V, and wich is at the same time:

1. "as straight as possible", that is "geodesic" in V;
2. an integral curve of the contact structure.

In general Γ will not be a straight line because it will have to satisfy the integrability condition. It will be "geodesic" *only in the class of integral curves*.

Mathematically, the problem is not trivial. We have to solve constrained Euler-Lagrange equations in the jet space V. We must first define appropriate Lagrangians on V based on

Riemannian metrics which reflect the weakening of the horizontal cortico-cortical connections when the discrepancy between the boundary values θ_A and θ_B increases. If the angle θ is measured relatively to the axis *AB* (θ has therefore an *intrinsic* geometric meaning), the weakening must vanish for $\theta = 0$ and $\theta = \pi$ and diverge for $\theta = \pi/2$. The function $p = f' = \tan\theta$ being the simplest function sharing this properties, it seems justified to test first the Euclidean metric of *V*. We will use a frame *Oxy* of *R* where the *x*-axis is identified with *AB*. The invariance under a change of frame is expressed by the action of the Euclidean group $E(2)$ on *V*.

We look therefore for curves of minimal length in *V among those which lift curves in R*, that is which satisfy the Frobenius integrability condition and are integrals of the contact structure. We will call them "Legendrian geodesics". Let $(x, y, p; \xi, \eta, \pi)$ be coordinates in the tangent space *TV* of *V*. We have to minimize the length of Γ expressed by the fonctional $\int_{x_A}^{x_B} ds$ where the element of arc length *ds* is given by $ds^2 = dx^2 + dy^2 + dp^2$. The energy to minimize is therefore $E = \int_{x_A}^{x_B} L(x)dx$ where the Lagrangien *L* is given, for a curve Γ of the form $(x, y = f(x), p = f'(x))$, by the formula $L(x)dx = ds$, that is by:

$$L(x) = \sqrt{\xi^2 + \eta^2 + \pi^2} = \sqrt{1 + f'(x)^2 + f''(x)^2}$$

We have to solve the Euler-Lagrange (E-L) equations constrained by the integrability constraint $p = f'(x)$, i.e. $\Sigma = 0$ with $\Sigma = p - \eta$. These constrained E-L equations are :

$$\begin{cases} \left(\dfrac{\partial}{\partial y} - \dfrac{d}{dx}\dfrac{\partial}{\partial \eta}\right)(L + \lambda\Sigma) = 0 \\ \left(\dfrac{\partial}{\partial p} - \dfrac{d}{dx}\dfrac{\partial}{\partial \pi}\right)(L + \lambda\Sigma) = 0 \end{cases}$$

where $\lambda(x)$ is a function, called a *Lagrange multiplier*. The idea is that the E-L equations with the constraint $\Sigma = 0$ are the same as the non constrained E-L equations for the modified Lagrangian $L + \lambda\Sigma$.

After some tedious computations, we get the following differential equations for the function $p = f'$, where *c* and *d* are two integration constants:

$$1 + p(x)^2 = (cp(x) + d)\sqrt{1 + p(x)^2 + p'(x)^2}$$

As the solution is given by an *elliptic integral,* Legendrian geodesics integrals of elliptic functions.

We can greatly simplify the solution of the equation when the function f is *even*, and the curve Γ *symmetric* under the symmetry $x \to -x$. Indeed, this condition implies immediately $c = 0$, whence, putting $k = 1/d$, the simpler differential equation for $p = f'$:

$$(p')^2 = \left(1 + p^2\right)\left[k^2\left(1 + p^2\right) - 1\right]$$

The parameter k is correlated to curvature: $k^2 - 1 = \kappa(0)^2$.

We get therefore:

$$x = \text{cst} + \int_0^{p(x)} \frac{1}{\sqrt{\left(1+t^2\right)\left(1 + \dfrac{k^2}{k^2-1}t^2\right)}}\,dt$$

which is a well known elliptic integral of the first kind.

We show in figure 17 how the solution f evolves when k varies from 1 to 1.65 by steps of 0.5.

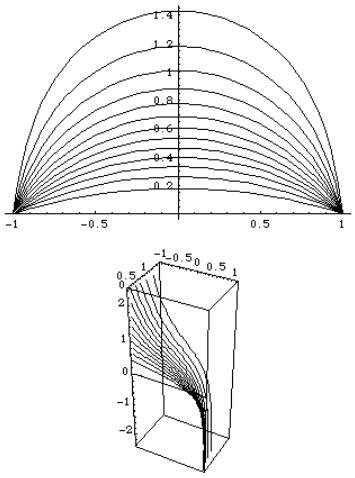

Figure 17. Evolution of Legendrian geodesics when the boundary tangents become more and more vertical. (a) Curves C in the base space R. (b) Curves Γ in the jet space V.

Figure 18 shows in the base space R and in the jet space V how the Legendrian geodesic corresponding to $k = 1.5$ is situated relatively to the arc of circle, the arc of parabola and the piecewise linear solution defined by the same boundary conditions.

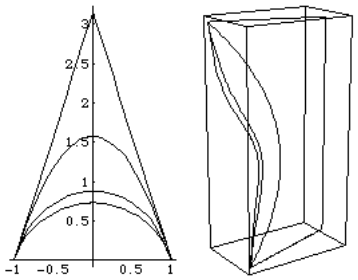

Figure 18. Position of the Legendrian geodesic ($k = 1.5$) relatively to the arc of circle, the arc of parabola and the piecewise linear solution defined by the same boundary conditions. (a) In the base space R. (b) In the jet space V.

The following table shows that the geodesic minimizes the length:

Curves	Geodesic	Arc of circle	Arc of parabola	Piecewise linear
	7.02277	7.04481	7.50298	12.9054

CONCLUSION

Due to the very strong geometrical structure of the functional architecture (hypercolumns, pinwheels, horizontal connections), the neural implementation of Kanizsa's contours is deeply linked with sophisticated structures belonging to what is called contact geometry and with variational models analogue to models already well known in physics.

BIBLIOGRAPHY

Bonhöffer, T., Grinvald, A., 1991: "Iso-orientation domains in cat visual cortex are arranged in pinwheel-like patterns", *Nature*, 353, 429-431.

Bosking, W., Zhang, Y., Schofield, B., Fitzpatrick, D., 1997: "Orientation Selectivity and the Arrangement of Horizontal Connections in Tree Shrew Striate Cortex", *J. of Neuroscience*, 17, 6, 2112-2127.

De Angelis, G., Ohzawa, I., Freeman, R., 1995: “Receptive Fields Dynamics in the Central Visual Pathways”, *Trends in Neuroscience*, 18, 451-458.

Dresp, B., Bonnet, C., 1995: “Subthreshold summation with illusory contours”, *Vision Research*, 35, 1071-1078.

Field, D., Hayes, A., Hess, R., 1993: “Contour Integration by the Human Visual System: Evidence for a Local ‘ Association Field ’”, *Vision Research*, 33, 2, 173-193.

Horn, B. K. P., 1983: “The curve of least energy”, *ACM Transactions in Mathematical Software*, 9, 4, 441-460.

Mumford, D., 1992: “Elastica and Computer Vision”, *Algebraic Geometry and Applications*, Springer.

Petitot, J., Tondut, Y., 1999: “Vers une neurogéométrie. Fibrations corticales, structures de contact et contours subjectifs modaux”, *Mathématiques, Informatique et Sciences Humaines*, 145, 5-101.

Spillman, L., Dresp, B., 1995: “Phenomena of illusory form~: can we bridge the gap between levels of explanation?”, *Perception*, 24, 1333-1364.

Ullman, S., 1976: “Filling-in the gaps: the shape of subjective contours and a model for their generation”, *Biological Cybernetics*, 25, 1-6 .